Melt Pool Size Control in Thin-Walled and Bulky Parts via Process Maps

Aditad Vasinonta, Jack L. Beuth and Raymond Ong
Department of Mechanical Engineering
Carnegie Mellon University
Pittsburgh, PA 15213

Abstract

Control of melt pool size is critical for maintaining consistent build conditions in the solid freeform fabrication of complex shapes. In this research, melt pool size in laser-based solid freeform fabrication processes is studied for both thin-walled structures and bulky parts. Numerical simulations are used to construct non-dimensional plots (termed process maps) that quantify the effects of changes in part height, laser power, deposition speed and part preheating on melt pool size. Strategies for the control of melt pool size suggested by the process maps are similar for the two geometries. Insights are given as to how transitions between these two extremes in geometry can be managed to maintain a consistent melt pool size. This modeling work is being performed in tandem with process development and melt pool imaging and control research underway on the LENS process at Sandia National Laboratories.

Nomenclature

T	= temperature in degrees Kelvin	T_m	= melting temperature
T_{base}	= base plate and wall preheat temperature	Q	= laser power
α	= fraction of laser power absorbed by the wall	V	= laser velocity
k	= thermal conductivity	ρ	= density
c	= specific heat	t	= wall thickness
L	= part length	h	= part height
W	= bulky part width	d	= melt pool depth
l	= melt pool length	w	= melt pool width

Introduction

A critical issue in developing solid freeform fabrication (SFF) processes as rapid manufacturing techniques is the control of "build conditions," defined as thermal conditions allowing a particular part to be fabricated. Consistency in build conditions is typically defined in terms of a consistent melt pool size during the construction of a part or feature. Previous work by the authors [1-3] has investigated this issue for 2-D thin-walled structures and has presented strategies for controlling build conditions (by maintaining a consistent melt pool size) while also limiting residual stresses (by controlling thermal gradients). The control of melt pool size and thermal gradients in 2-D thin-walled structures was addressed via three-dimensional plots of dimensionless process variables (termed process maps) developed from thermal models of laser-based material deposition.

Current research extends the process map concept developed for 2-D thin-walled structures to 3-D bulky parts. A process map for melt pool size for bulky parts has been

developed through thermal simulations of a simple 3-D structure. It addresses the effect of changes in process variables (laser power, laser velocity and part preheat temperature) and geometry (part height) on melt pool size. Comparing the process maps for thin-walled and bulky structures provides insight into how to control melt pool size for these two extremes in geometry and how to handle transitions between them in a single part. Furthermore, an understanding of these two basic types of structures can form the basis for understanding process control issues in the building of much more complex shapes.

The principal application of this work is to the Laser Engineered Net Shaping (LENS) process currently under development at Sandia National Laboratories [4]. The process maps presented in this paper have been developed to aid in both manual and automated process control efforts currently underway at Sandia Labs [5]. Although this research is directed toward the LENS process, the approach taken is applicable to any solid freeform fabrication process involving a moving heat source. Similarly, although stainless steel (SS304) is treated in the current work, the same approach can be applied to other materials.

In the next section, the 2-D and 3-D structures analyzed in this study are presented, along with details of the finite element models and boundary conditions used. Nondimensionalization schemes used to develop the process maps for both geometries are given. In the succeeding section, the process maps are presented with rules for how results can be applied to the prediction and control of melt pool size. A comparison of melt pool sizes between the two geometries is then presented. Finally, process control-related insights for transitions between the two geometries are discussed.

Geometry Considered, Numerical Model and Analytical Solution

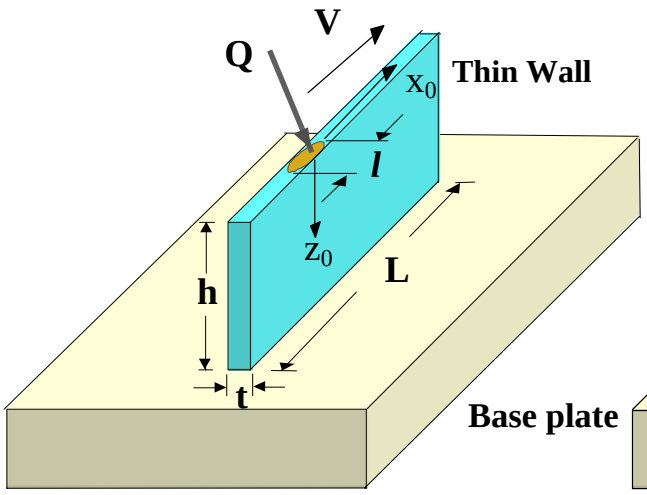

Figure 1a. Thin-Walled Structure

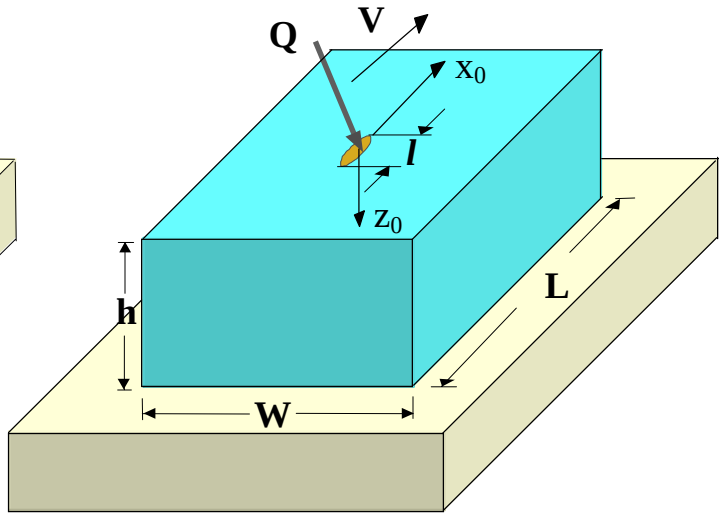

Figure 1b. Bulky Part

Schematics of both the thin-walled and bulky part geometries are shown in Fig. 1. In the LENS process, parts are constructed by focusing a high power laser onto a metal substrate, where streams of metallic powder are simultaneously injected. The laser locally melts the powder to form a molten melt pool on the top surface of the growing part. By moving the laser beam, the material is added to the part and the part is built up line-by-line and layer-by-layer.

In the modeling of this study, it is assumed that both the thin-walled and bulky parts are fabricated on large fixed-temperature metallic substrates, which act as thermal heat sinks. Models are also constructed such that the distance traveled by the laser and the length of the structures in the x-direction are large enough that steady state thermal conditions exist at the melt pool. Numerical models used in this study do not include the effect of convective heat transfer from the wall free surfaces to the surrounding air and do not model convective flows in the melt pool itself. Work by Dobranich and Dykhuizen [6] suggests strongly that the role of these effects in determining melt pool size is not significant. The models of this study also represent the laser as a point source of heat, neglecting the distribution of laser power over the melt pool region. Assuming a point source of power is reasonable given the goal of this study, which is to capture *changes* in melt pool size and other parameters as a function of *changes* in the process variables outlined above. Accuracy in the absolute predictions is of secondary importance. However, comparisons between experimentally determined melt pool sizes for thin-walled structures and model predictions show reasonable agreement [3].

The meshes and boundary conditions used for typical 2-D thin-walled and 3-D bulky part thermal models are shown in Figs. 2 and 3 respectively. For both geometries, a concentrated heat source moves across the top surface of the model, which is initially at a uniform temperature $T = T_{base}$. The finite element models have been created using the ABAQUS software package. Because of high temperature gradients in the region near heat source, the grid of each model is biased toward the region that will surround the heat source at the time when results are to be extracted from the model. In addition to comparisons with analytical solutions valid for large substrates, the convergence of each mesh was checked against a model with roughly half the resolution with no noticeable change in the results.

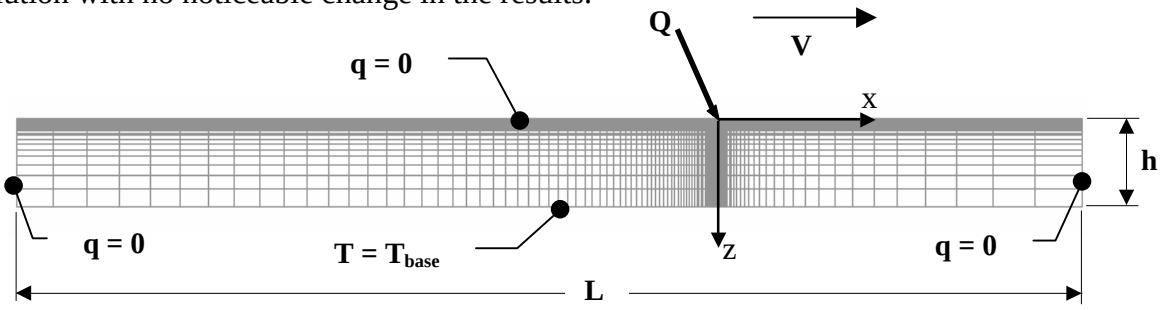

Figure 2. 2-D Thermal Model and Boundary Conditions

For the case of a thin-walled structure, four-noded bilinear thermal elements were used to form the mesh of the 2-D model. It is assumed that the thin wall is fabricated by depositing material along a single row; thus, the thickness of the wall is comparable to the melt pool size. As illustrated in Fig. 2, an insulated boundary condition is imposed on the top and both vertical sides of the substrate. Sensitivity studies have shown that thermal results are not significantly affected by boundary conditions along these surfaces being specified as either insulation or convection. By using a 2-D model, it is also assumed that there is no heat loss through the front and back surfaces. The temperature along the substrate bottom is specified as fixed at the value equal to the temperature of the base plate.

A typical mesh for a 3-D bulky part simulation is shown in Fig. 3, generated using eight-noded linear brick thermal elements. Because of symmetry across the X_0-Z_0 plane, only half of

the 3-D structure is modeled. Analogous to the 2-D model, insulated boundary conditions are imposed on all free surfaces. The heat flux across the symmetry plane (the X_0-Z_0 plane) is set to zero and the temperature of the substrate bottom is held at the temperature of the base plate.

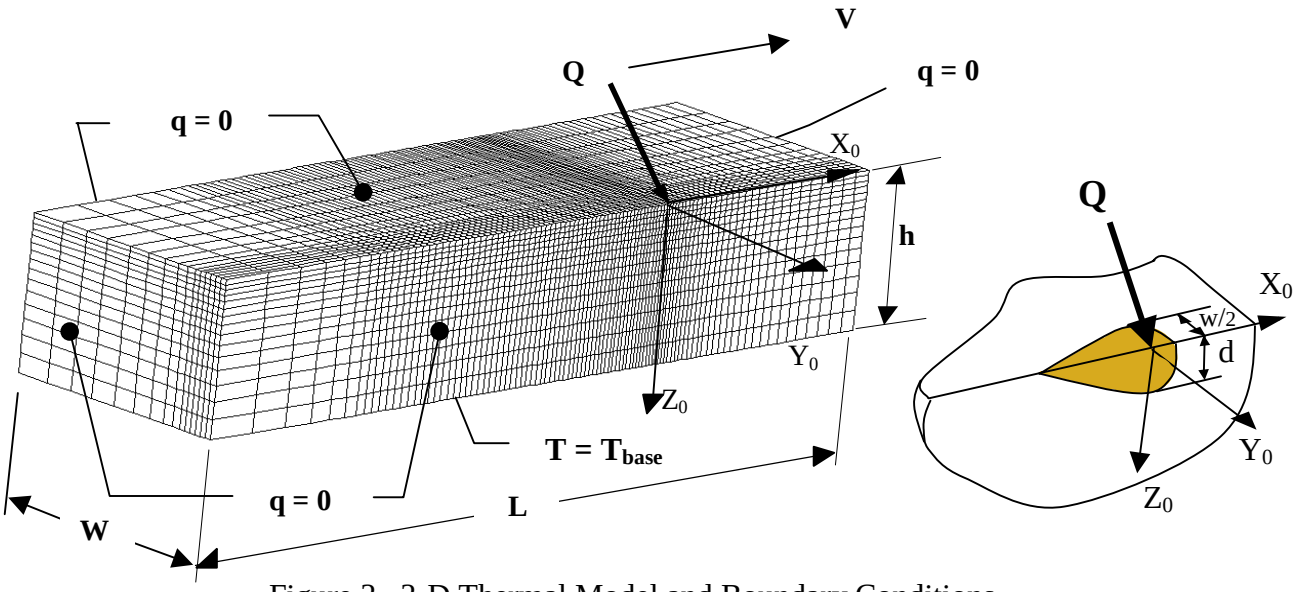

Figure 3. 3-D Thermal Model and Boundary Conditions

Thermal properties of AISI 304 stainless steel (SS304), which is used in the LENS and other SFF metal deposition processes, are used as inputs for the temperature-dependent simulations. Thermal properties were taken from [7] and are also comparable to those used by Chin, et al. [8] and Klingbeil, et al. [9] in thermomechanical modeling of the Shape Deposition Manufacturing process. The properties used in the model that are set to depend on temperature are specific heat and thermal conductivity. The latent heat of the liquid-solid phase transition is also included in the model.

The normalization schemes used to develop process maps in this paper are based on the analytical solutions of conductive heat transfer by Rosenthal [10]. Representation of numerical simulation results in terms of the normalized variables defined below is exact only in the case of temperature-independent thermal properties. The goal of developing process maps for laser-based SFF processes is to use dimensionless variables to collapse a large number of numerical simulations into an easily used format, keeping errors caused by temperature dependent properties within acceptable limits. As suggested by the Rosenthal solution for a point source of heat moving across a 2-D semi-infinite thin substrate, a process map for melt pool size for a thin-walled structure is represented through three dimensionless variables: the normalized melt pool length ($\bar{l}$), the normalized height of the substrate ($\bar{h}$) and the normalized melting temperature ($\overline{T}_m$), which are defined as follows:

$$\bar{l} = \frac{l}{2k/\rho cV}, \qquad \bar{h} = \frac{h}{2k/\rho cV} \qquad \text{and} \qquad \overline{T}_m = \frac{T_m - T_{base}}{\alpha Q/\pi k t}. \tag{1}$$

Using this normalization scheme, results for normalized melt pool length, $\bar{l}$, are presented as a function of normalized wall height, $\bar{h}$, and normalized melting temperature, $\overline{T}_m$.

Analogous to the case of a 2-D thin wall, the 3-D conductive heat transfer solution by Rosenthal suggests that the process map for melt pool size of a bulky part can be represented by three dimensionless variables: the normalized melt pool depth ($\bar{d}$), the normalized height of substrate ($\bar{h}$) and the normalized melting temperature ($\bar{T}_m$). The melt pool depth is chosen to represent the size of melt pool for 3-D bulky parts because it can be related to how well newly deposited material is fused to the top surface of the part. The dimensionless variables for the process map for bulky parts are defined as follows:

$$\bar{d} = \frac{d}{2k/\rho cV}, \qquad \bar{h} = \frac{h}{2k/\rho cV} \qquad \text{and} \qquad \bar{T}_m = \frac{T_m - T_{base}}{\left(\alpha Q/\pi k\right)\left(\rho cV/2k\right)}. \tag{2}$$

Note that the normalized melting temperature ($\bar{T}_m$) for the two geometries is defined differently.

Process Map for 2-D Thin-Walled Structures

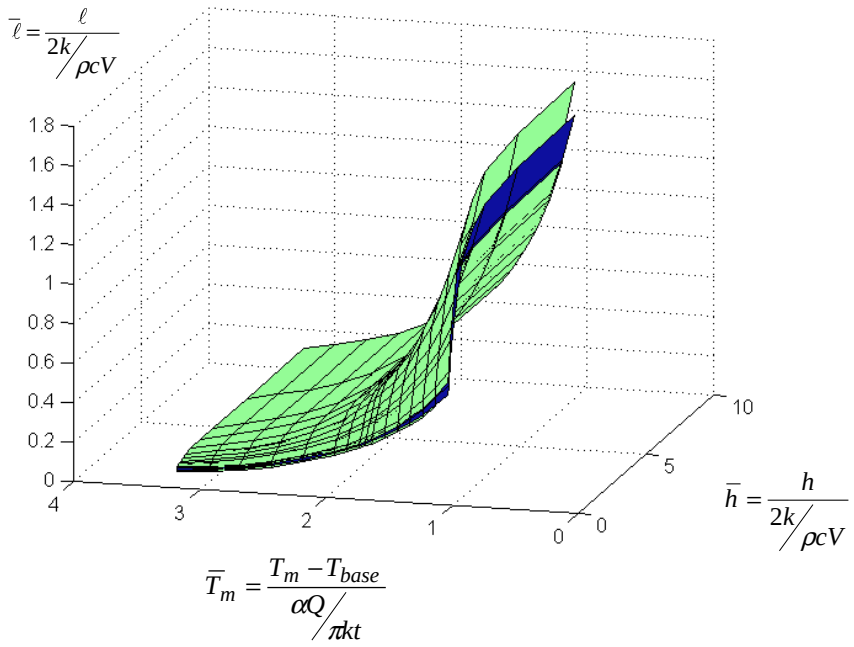

Figure 4. Process Map for Melt Pool Length for 2-D Thin-Walled Structures

A process map for melt pool length for a thin-walled structure with a concentrated laser heat source moving across it has been developed and reported in [1-3]. The work described in [1] uses slightly different normalization rules than the more accurate rules used in [2], [3] and herein. The process map, which is shown in Fig. 4, consists of three surfaces plotted on three coordinate axes. The middle surface was developed from several numerical simulations with temperature-independent properties performed with differing wall heights in order to get the dependence of $\bar{l}$ on $\bar{h}$. The dependence of $\bar{l}$ on $\bar{T}_m$ was then determined from the same simulations by assuming different values of T_m. The results from temperature-dependent simulations are also represented in Fig. 3 by upper and lower surfaces that bound the temperature-independent results. The space between these surfaces reflects the range in results seen when process variables are varied over the range of specific interest in the LENS process.

That range consists of values of αQ from 43.2 to 165 W, V from 5.93 to 9.31 mm/sec and T_{base} from 30° C to 400° C. The maximum range in values of $\bar{l}$ for fixed $\bar{h}$ and $\overline{T_m}$ due to the temperature dependence of properties is less than 13% of the nominal value of $\bar{l}$. Thus if the mean values of $\bar{l}$ for a fixed value of $\overline{T_m}$ are consistently used, the maximum error is ± 6.5%.

The detailed assumptions and procedures for obtaining and using the process map for melt pool length are given in [3]. In brief, the process map of Fig. 4 can be used effectively for SS304 deposition within the range of process parameters of interest in the LENS process by applying the following four rules:

1. Properties of SS304 at 1000 K are used in the normalization;
2. For cases involving a change in preheat, a linear change in thermal conductivity with a preheat temperature is assumed, as given in the following equation,
$$k = 24.3 + 0.013\left(T_{base} - 30\right) \qquad W/(mK); \tag{3}$$
3. For predicting steady-state melt pool lengths due to a change in process variables, wall thickness is assumed to scale proportionally with melt pool length; and
4. It is assumed that the melt pool length/wall thickness scaling is unaffected by velocity.

Melt pool sizes determined by real-time thermal imaging experiments [5] have been compared with model predictions using the process map of Fig. 4 and the rules outlined above [3]. Reasonable agreement is seen in melt pool length values and the predictions of the process map clearly capture the trends in the measured results.

Process Map for 3-D Bulky Structures

In this section, results are presented from modeling the LENS process for deposition of SS304 to form 3-D bulky parts. The normalization scheme for 3-D structures given in eq. (2) is used. The process map has been developed using concepts similar to those used for 2-D thin-walled structures; however, melt pool depth is chosen to be the parameter representing melt pool size instead of melt pool length. Melt pool depth is chosen because it determines how much of the top of the existing layer is melted by a newly deposited layer. In laser-based SFF processes, controlling melt pool depth as a part is built is important for ensuring fusion at interlayer boundaries. If the melt pool depth is too small, not enough of the top portion of the existing material will be melted during deposition and poor interlayer bonding will result.

Although it is important to control melt pool depth to ensure part quality, it is a difficult parameter to monitor by thermal imaging or other methods. However, the 3-D Rosenthal solution for a point heat source moving across a semi-infinite substrate suggests that, for a tall bulky part, the depth of the melt pool is identical to one half of the width of the melt pool, independent of laser power, laser velocity and preheat temperature. Thus for tall parts, melt pool widths measured via thermal imaging techniques can be compared directly to predicted melt pool depths. Also, it is planned to use thermal model results to quantify the ratio of melt pool width to melt pool depth as a function of part height, to facilitate the use of real-time thermal images of melt pool width to precisely control melt pool depth. It should be noted that it is also possible to relate melt pool areas, which are easily extracted from thermal images, to melt pool depths. However, if changes in laser velocity are allowed, the ratio of melt pool area to

melt pool depth will be a function of laser velocity, laser power and preheat temperature in addition to part height. Because of this, melt pool width is generally a more useful measurable parameter to control as a means for controlling melt pool depth.

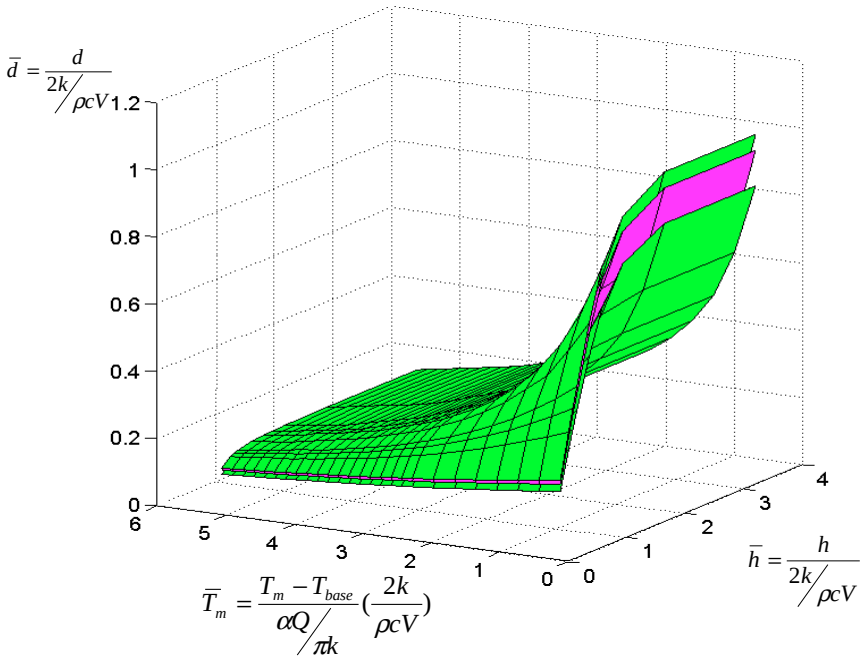

Figure 5. Process Map for Melt Pool Depth for 3-D Bulky Structures

The process map developed for 3-D bulky parts (shown in Fig. 5) consists of three surfaces plotted on three coordinate axes, generated using several numerical models with different part heights. Similar to the process map for 2-D thin-walled structures, the middle surface is generated from simulations assuming temperature-independent properties. Within the limitation of this assumption, this surface is very general and is applicable to any laser-based SFF process involving thermal deposition of any single material. The two bounding surfaces developed from temperature-dependent simulations reflect the range in results seen when process variables are varied over the range of practical use in the LENS process.

As for the process map for thin-walled structures, results from temperature-dependent simulations are normalized using the properties of 304 stainless steel at 1000 K, with the linear change in thermal conductivity as given in eq. (3) applied for cases involving a uniform preheat. The maximum range in values of $\bar{d}$ for fixed $\bar{h}$ and $\bar{T}_m$ is 16% of the nominal value of $\bar{d}$. Thus if the mean values of $\bar{d}$ for a fixed value of $\bar{T}_m$ are used, the maximum error is ± 8%, which is slightly higher than the range of melt pool lengths ($\bar{l}$) for the process map for 2-D thin-walled structures. If properties at 1100 K are used to normalize the 3-D results, maximum errors can be further reduced to approximately ± 6.5%. However, use of the same normalization scheme for both thin-walled and bulky parts offers advantages in comparing melt pool sizes between the two geometries and in understanding transitions between them.

It can be seen in both Figs. 4 and 5 that for a fixed value of $\bar{h}$, melt pool size ($\bar{l}$ for a 2-D thin wall and $\bar{d}$ for a 3-D bulky part) increases with increasing T_{base} or Q (either of which

decreases $\overline{T}_m$). Moreover, a change in T_{base} can be compensated for by a change in Q, to retain a desired melt pool size. When the part is relatively tall, the fixed temperature at the base is not seen at the melt pool, $\overline{h}$ has no significant effect on the size of melt pool, and the results approach those for an infinitely large part. In contrast, $\overline{h}$ has a considerable effect on melt pool size when the part is relatively short, with $\overline{d}$ and $\overline{l}$ dropping rapidly as $\overline{h}$ is reduced.

When comparing melt pool sizes for the two extreme geometries, it is found that, for the same set of process variables, melt pool sizes extracted from the process map for 3-D bulky parts are much smaller than those extracted from the process map for 2-D thin-walled structures. For example, for a tall, thin wall, using typical process variables of αQ = 105 W, V = 7.6 mm/s, and T_{base} = 303 K (and a wall thickness of 1.3 mm) the melt pool length calculated from the process map is equal to 1.4 mm. For the same process variables, the melt pool depth and melt pool length for a tall, 3-D bulky part are found to equal 0.40 mm and 0.85 mm respectively. The considerable difference in melt pool lengths between the two geometries (1.4 mm and 0.85 mm) is due to the fact that there is more material to conduct heat away from the melt pool in the 3-D bulky part.

To keep melt pool size constant while transitioning from thin-walled to bulky features, laser power must be increased. For the case considered above, to obtain a melt pool size of 1.4 mm in a bulky feature, the absorbed laser power must be increased from 105 W to 160 W. Decreasing laser velocity and using part preheating can also increase melt pool size; however, these measures cannot be used alone. Within the practical range of laser velocity and part preheating in the LENS process, melt pool size changes from each of these process changes are not large enough to regain the thin-walled feature melt pool size.

Conclusions

In this paper, process maps have been presented for predicting and controlling melt pool size in the building of thin-walled and bulky stainless steel structures by laser-based SFF processes. For each of the two geometries, all numerical model predictions have been collapsed onto a single three-dimensional plot of dimensionless process variables. The process map for bulky parts could have been made more accurate by developing normalization rules specifically for that geometry; however, both process maps presented herein use the same normalization rules, making a direct comparison between the geometries easier. The process map for bulky parts quantifies values of melt pool depth, which is the key parameter to control for consistent build conditions. Although melt pool area is typically tracked in bulky parts via thermal imaging measurement and control systems, melt pool width is a better parameter to monitor experimentally, due to its more direct link to melt pool depth.

A comparison of melt pool sizes between the two geometries shows that, for the same set of process variables, the size of the melt pool decreases substantially when transitioning from thin-walled to bulky features (decreasing by 39% in the example cited herein). To maintain consistent build conditions, decreasing the laser velocity or base plate preheating alone is not sufficient and a substantial increase in laser power is needed (a 52% increase in the cited example). A detailed comparison of predictions from the two process maps (not presented in this paper) reveals that most process control-related insights and implications relevant to 2-D thin-walled structures also apply to 3-D bulky parts. For example, practical levels of uniform part

preheating, which is pursued as a means to decrease residual stresses, does not increase melt pool sizes significantly for either geometry. Furthermore, any increase in melt pool size can be eliminated by a small decrease in laser power or increase in laser velocity. It is also clear from both process maps that considerably smaller melt pool sizes are seen for short structures. Thus control of melt pool size as a part is built up from a base plate is important. Because it does not significantly change melt pool size, base plate preheating is not sufficient to address this problem.

Acknowledgements

This research has been supported by the National Science Foundation under grant DMI-9700320 and by Sandia National Laboratories under grant BE-0792. The authors would like to than Michelle Griffth of Sandia National Laboratories, Albuquerque, NM, for her substantial collaboration on this research.

References

1. Vasinonta, A., Beuth, J.L. and Griffith, M., "Process Maps for Laser Deposition of Thin-Walled Structures," *Solid Freeform Fabrication Proceedings*, D.L. Bourell, J.J. Beaman, R.H. Crawford, H.L. Marcus and J.W. Barlow, eds., The University of Texas at Austin, August 1999, pp. 383-391.
2. Vasinonta, A., Beuth, J.L. and Griffith, M., "Process Maps for Controlling Residual Stress and Melt Pool Size in Laser-Based SFF Processes," *Solid Freeform Fabrication Proceedings*, D.L. Bourell, J.J. Beaman, R.H. Crawford, H.L. Marcus and J.W. Barlow, eds., The University of Texas at Austin, August 2000, pp. 200-208.
3. Vasinonta, A., Beuth, J.L. and Griffith, M., "A Process Map for Consistent Build Conditions in the Solid Freeform Fabrication of Thin-Walled Structures," *Journal of Manufacturing Science and Engineering*, in print.
4. Griffith, M.L., Keicher, D.M., Atwood, C.L., Romero, J.A., Smugeresky, J.E., Harwell, L.D. and Greene, D.L., "Freeform Fabrication of Metallic Components Using Laser Engineered Net Shaping (LENS)," *Solid Freeform Fabrication Proceedings*, D.L. Bourell, J.J. Beaman, H.L. Marcus, R.H. Crawford and J.W. Barlow, eds., The University of Texas at Austin, August 1996, pp. 125-132.
5. Griffith, M.L., Schlienger, M.E., Harwell, L.D., Oliver, M.S., Baldwin, M.D., Ensz, M.T., Smugeresky, J.E., Essien, M., Brooks, J., Robino, C.V., Hofmeister, W.H., Wert, M.J. and Nelson, D.V., "Understanding Thermal Behavior in the LENS Process," *Journal of Materials Design*, Vol. 20, No. 2/3, 1999, pp. 107-114.
6. Dykhuizen, R.C. and Dobranich, D., "Analytical Thermal Models for the LENS Process," Sandia National Laboratories Internal Report, 1998.
7. Dobranich, D. and Dykhuizen, R.C., "Scoping Thermal Calculation of the LENS Process," Sandia National Laboratories Internal Report, 1998.
8. Chin, R.K., "Thermomechanical Modeling of Residual Stresses in Layered Manufacturing with Metals," Ph.D. Thesis, Carnegie Mellon University, May 1998.
9. Klingbeil, N.W., Beuth, J.L., Chin, R.K. and Amon, C.H., "Measurement and Modeling of Residual Stress-Induced Warping in Direct Metal Deposition Processes," *Solid Freeform Fabrication Proceedings*, H.L. Marcus, J.J. Beaman, D.L. Bourell, J.W. Barlow and R.H. Crawford, eds., The University of Texas at Austin, August 1998, pp. 367-374.
10. Rosenthal, D., "The Theory of Moving Sources of Heat and Its Application to Metal Treatments," *Transactions of the ASME*, Vol. 68, 1946, pp. 849-866.